

Controlling a vehicle braking and longitudinal acceleration using a seeking control approach

Saad A. Salman¹, Abidaoun H. Shallal², Ahmad H. Sabry³

¹Department of Computer Engineering, College of Engineering, University of Diyala, Baqubah, Iraq

²Department of Communication Engineering, College of Engineering, University of Diyala, Baqubah, Iraq

³Department of Computer Engineering, College of Engineering, Al-Nahrain University, Baghdad, Iraq

Article Info

Article history:

Received Dec 27, 2022

Revised Mar 24, 2023

Accepted Apr 17, 2023

Keywords:

Adaptive cruise control
Braking control
Extremum seeking technique
Longitudinal control
Vehicle speed and spacing
controller

ABSTRACT

Traditional methods for tracking the paths of driverless vehicles use plant models to determine the corresponding control laws. Due to the intricate interactions between the road and the tires, time-varying characteristics, and unidentified disturbances. It is challenging to create an accurate vehicle model. As a result, data-driven controllers, which are independent of a predetermined plant model are becoming more and more well-liked. This work implements adaptive cruise control (ACC) by employing a control approach called extremum seeking technique (EST), which is a model-free control (MFC), to control a vehicle braking and longitudinal acceleration. The main aim here is to create an ego vehicle that travels at a specific speed with maintaining a secure space with respect to a guide vehicle. A car including an ACC technique called ego car, exploits radar to determine relative velocity and relative space relating to the guiding car. The ACC technique is considered to keep maintain a relatively secure space or a preferred cruising velocity concerning the guiding vehicle. The developed model succeeded to determine the relative velocity and relative space according for the ego car to another guiding car with acceleration not more than ± 2 m/s² and spacing error less than 6 m.

This is an open access article under the [CC BY-SA](#) license.



Corresponding Author:

Ahmad H. Sabry
Department of Computer Engineering, College of Engineering, Al-Nahrain University
Al Jadriyah Bridge, Baghdad, Iraq
Email: ahs4771384@gmail.com

1. INTRODUCTION

In today's technologically advanced world, it is becoming more and more important to create intelligent composing systems that are capable of carrying out various control duties. As a result, the connectivity between these units also becomes crucial. Therefore, it is crucial to accurately design the compositional systems that control these linkages. Each component of this compositional design should function as predicted without concern for any intervention that would impair the overall performance of the system. Traditional methods for tracking the paths of driverless vehicles use plant models to determine the corresponding control laws. Due to the intricate interactions between the road and the tires, time-varying characteristics, and unidentified disturbances. It is challenging to create an accurate vehicle model. As a result, data-driven controllers [1]–[3], which are independent of a predetermined plant model are becoming more and more well-liked. Particularly, the model-free control (MFC), which offers a simple solution to earth vehicle pathway tracking, characterizes the derivatives of an output control as summations of an offset term and an amplified control input. Despite its simplicity, MFC still largely relies on trial-and-error tweaking for control gain, which can be tedious and unreliable.

Smart energy systems, smart medical equipment, and smart transportation systems are a few examples of cyber-physical systems [4], [5]. These systems essentially have two main components: i) a physical component that gives the system a continuous representation of the physical world, typically through the use of ordinary differential equations and ii) a communication and computational component that keeps an eye on, coordinates, and controls the physical systems. Strong communication links are necessary for the computing unit, which also houses the design's software component, to both receive and transmit data to the outside world [6]. Cyber-physical systems control and robustness and reliability maintenance face enormous hurdles. Dissipativity and more precisely passivity are energy-based notions that offer a potent tool for overcoming the difficulties that compositional systems bring about. Instead of producing their energy, passive systems merely store or release the energy that has been supplied to them. For zero-state detectable (ZSD) systems, passivity can exhibit asymptotic stability in the proper circumstances [7]. Passivity and stability are maintained for large-scale systems made up of passive stable units because both negative feedback and parallel interconnections of passive systems remain passive [8]. Because of this, passive designs are an excellent choice for developing cyber-physical systems. An important variable in vehicle safety control systems is the tire-road friction coefficient. Antilock braking systems (ABS) and traction control systems (TCS) in particular need friction information when braking and when accelerating. The road condition determines the extremum of the force characteristic acting on the tires. Extremum seeking technique (EST) is a real-time model-free adaptive control method used to adapt parameters to unidentified mappings and unidentified system dynamics starting by input parameters to the objective function. EST can solve dynamic systems problems related to parameters and static optimization [9], [10].

The adaptive gain-tuning techniques now in use either rely on the attempt to simultaneously recognize the offset term and the control gain or the directive from the previous step to repeatedly renew the control gain at the present phase. They might, however, result in chattering or unrestricted improvements in control. Research by Wang *et al.* [9] integrated a MFC with the EST to offer a fresh perspective for the MFC gain adjustment while enhancing its control performance for the EST. To gradually improve the control performance of the MFC, EST changes the control gain of real-time MFC. However, the stability of the method was not effective for vehicle braking and longitudinal acceleration. The adaptive constant wheel slip control (WSC) for exercise service vehicles with decoupled high-dynamic electro-hydraulic brake systems was described in [11]. Although this study describes the system design and a mathematical formulation of the WSC was proposed as a state estimator, the presented algorithm didn't discuss vehicle braking. This issue has been discussed by Zhou *et al.* [12] with a new fractional-order EST method based online but for another application, which is an energy management control application. Research by Lin *et al.* [13] proposed a method without using position measurements by addressing a 3-D problem involving maneuvering a nonholonomic vehicle to locate an unidentified source of a spatially distributed signal field. An EST-based method with configurable pitch, yaw velocities, and constant forward speed was presented. However, the longitudinal acceleration didn't consider the control loop. Research by See *et al.* [14] solved the boundary layer thickness of the water column for an underwater vehicle. Although this study presented an EST-based unscented Kalman filter detecting and tracking this cannot be applied on a ground vehicle. Research by Zengin *et al.* [15] developed an EST based on recursive least squares to determine the ideal slip ratio online to achieve the greatest acceleration/deceleration. Although the presented simulation results demonstrated the efficacy of the created method and quantitatively compare it with a gradient-based estimate, there is no discussion about the breaking control of the vehicle. Research by Liu *et al.* [16] presented EST on a Hammerstein plant together with an adaptive phase compensator and a high-gain optimizer. However, this system didn't present a safety distance and braking controller. Research by Bhattacharjee *et al.* [17] examined two methods: i) the peak seeking algorithm based on adaptive sampling and ii) the EST. The nonlinear model predictive controller (MPC) uses a brand-new state dependent coefficient version of the nonlinear quadcopter dynamics. This makes it possible to include input, state, and output constraints in the formulation, which increases the realism of the simulations. The suggested algorithms were effective in locating the area of greatest concentration for a constant plume but not for tracking, safe distance, and breaking control.

All this allows asserting that it is expedient to conduct a study on implementing an adaptive cruise control (ACC) by employing an EST control approach to control a vehicle braking and longitudinal acceleration, which will lead to creating an ego vehicle that travels at a specific speed with maintaining a secure space with respect to a guide vehicle. The aim of the research is to implement ACC by employing a control approach called EST to create an ego vehicle that travels at a specific speed with maintaining a secure space with respect. This will make it possible to a guide vehicle using braking and longitudinal acceleration control. To achieve this aim, the following objectives are accomplished: i) to obtain the velocity and relative space for the guide and ego vehicles, ii) to examine EST seeking cost function, and iii) to analyze and get the gains of controllers during tracking simulation.

2. METHOD

2.1. Object and research hypothesis

This work develops an implementation of ACC by employing a control approach called EST. A car including an ACC technique called ego car exploits radar to determine relative velocity (V_{rel}) and relative space (S_{rel}) relating to the guiding car. The ACC technique is considered to preserve and maintain a relatively secure space (S_{saf}) or a preferred cruising velocity (V_{set}) from the guiding vehicle. The control objective is settled according to the following circumstances:

- If $S_{rel} > S_{saf}$, the ACC will follow the preferred reference cruise speed that the driver is controlling.
- If $S_{rel} < S_{saf}$, the ACC will control the ego vehicle's relative location with regard to the guide vehicle.

2.2. Using adaptive cruise control

In this work, we use the same ACC technique with MPC to model both the guide and ego vehicle using MATLAB environment functions. The assumptions made in the work are described in section 2.4, while the simplifications adopted are demonstrated in the following subsections. By implementing a simple second-order linear model [18], the longitudinal dynamics of the vehicle can be represented by the following transfer function:

$$G = \frac{1}{0.5s^2 + s} \quad (1)$$

where the parameters of the ACC are listed in Table 1.

Table 1. Adaptive cruise control parameters

Description	Value	Description	Value
Default spacing (m)	D_default=10	Maximum acceleration for driver comfort (m/s ²)	amax_ego=2
Time gap (s)	t_gap=1.4	Minimum acceleration for driver comfort (m/s ²)	amin_ego=-3
Initial ego car velocity (m/s)	v0_ego=20	Driver-set velocity (m/s)	v_set=30
Initial ego car position (m)	x0_ego=10	Sample time (s)	Ts=0.1
Initial lead car velocity (m/s)	v0_lead=25	Duration (s)	Tf=150
Initial lead car position (m)	x0_lead=50		

2.3. Applying extremum seeking technique with adaptive cruise control

To maximize an objective function, EST is used to tune the parameters of the controllers that are adaptive MFC [19]. These controllers are functional to be adapted to unknown mappings from an objective function to control parameters and unidentified system dynamics. The EST employs a different tuning loop for each parameter when searching for several parameters. By perturbing (modulating) the parameters with a sinusoidal signal and demodulating the resultant perturbed goal function, the EST block looks for the best control parameters. Figure 1 demonstrates the block diagram of applying the EST with ACC.

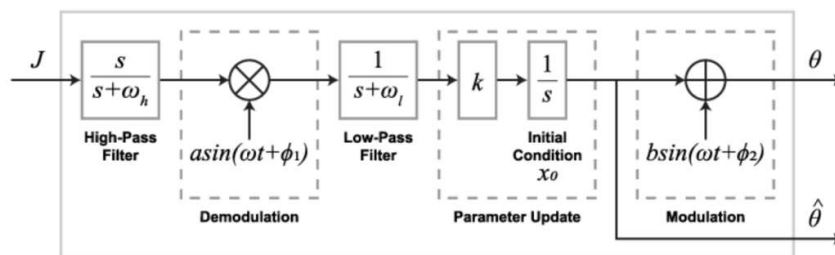


Figure 1. Applying extremum seeking technique

Referring to the Figure 1, ω_l and ω_h denote the low-pass filter and the high-pass filter cutoff frequency, respectively. T_s denotes the discrete-time controller sample time learning rate. The θ and $\hat{\theta}$ denote the modulation and estimated parameter of the signal, while $y = f(\theta)$ represents the optimized objective function output with forcing frequency (ω) for the demodulated ($a \cdot \sin(\omega t)$) and modulated ($b \cdot \sin(\omega t)$) signals on the k learning rate. At the highest value of $f(\theta)$, the parameter's ideal value, θ^* , occurs. We use a different tuning loop for each parameter to optimize several parameters. The EST for a

growing segment of the objective function plot is shown in Figure 2(a). The modulated waveform is made up of the existing predictable parameter and the modulation waveform. A perturbed objective function of the same stage as the modulation waveform is produced by applying $f(\theta)$. A positive signal is generated by multiplying the demodulation signal by the altered objective function. The value rises as the signal is integrated, bringing it closer to the objective function's peak. The goal function curve's declining section is illustrated as EST in Figure 2(b).

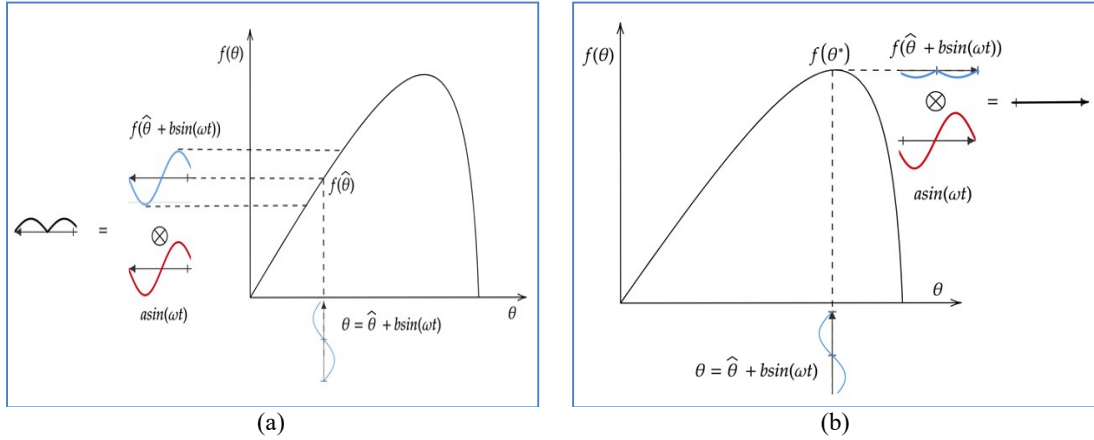


Figure 2. EST for; (a) a growing segment and (b) a declining section of the objective function plot

Applying $f(\theta)$ in this situation results in 180° out of phase objective function with the modulation waveform. A negative signal is generated by multiplying the demodulation signal [20]. To construct an EST algorithm, we configure parameter initial conditions, learning rates, demodulation signal, modulation signals, and appropriate forcing frequencies. Then set the time scale to the fastest value is ensured for the system dynamics, a medium time scale for the perturbation forcing frequencies, and the slowest time scale for the filter cutoff frequencies. EST can be used in both discrete-time and continuous-time systems. The tuning loops include the time domain of the integrators, low-pass filters, and high-pass filters are all impacted by a change in the controller's time domain. We use a discrete-time controller to provide code for the EST, which can be deployed on the hardware. By modifying control settings in real-time to optimize an objective function (J), EST achieves sufficient control performance [21]–[23]. We use this objective function, which is dependent on set velocity, relative velocity, safe distance, and relative distance, J for this work can be represented as in (2):

$$J = -\int Q_d(S_{rel} - S_{saf})^2 + Q_d(v_{rel} - v_{set})^2 \quad (2)$$

Here $Q_v = 0.5$ and $Q_d = 1$ are the weights of the objective function of the velocity error and distance error index. EST tunes the values of the parameters by using the following phases:

- The modulation stage uses a low-amplitude sinusoidal signal to change the value of the parameter being improved.
- Response stage, where the optimizing system responds to the perturbations of the parameter, that response may affect an equivalent transform on the value of the objective function.
- The demodulation stage multiplies a sinusoidal signal of a frequency similar to the modulation signal by the objective function signal. To eliminate bias from the objective function waveform, this phase contains a high-pass filter as an option.
- Updating the parameters stage, this process performs an integration process and optional low-pass filter on the demodulated input signals to eliminate the noise of high-frequency. The state of the integrator represents the parameter value.

The EST considers the position error gain (K_{xerr}), velocity error gain (K_{verr}), and relative velocity gain (K_{vrel}) as the gains for the EST controller [24]. These gains are specified initially with values 1, 1, and 0.5, respectively for the ACC.

2.4. Identifying parameters of extremum seeking technique

The three gains of these controllers have been tuned by specifying the number of parameters ($N = 3$). Each parameter is tuned using a different tuning loop by the controller. By amounting the preliminary gain values regarding the learning rate for every parameter lr , we specify the parameter initial conditions for updating integrators by $lr = 0.02[2,3,1]$ and set the frequencies, phases, amplitudes of the modulation, and demodulation signals (ϕ_2 , ϕ_1 , and ω) (b and a). There must be a different forcing frequency for each parameter. In this work, we use identical demodulation, modulation amplitudes, and phases for all parameters. A low-pass filter eliminates the noise due to the high frequency from the demodulated input, a high-pass filter is used to eliminate the signal bias of the anxious goal function and to give these filters their cut-off frequencies. The simulation of the EST-based ACC is shown in Figure 3, while the objective and plant dynamics block that computes the objective function and includes the ACC models for the ESC method is shown in Figure 4. The parameters of the extremum-seeking technique are listed in Table 2.

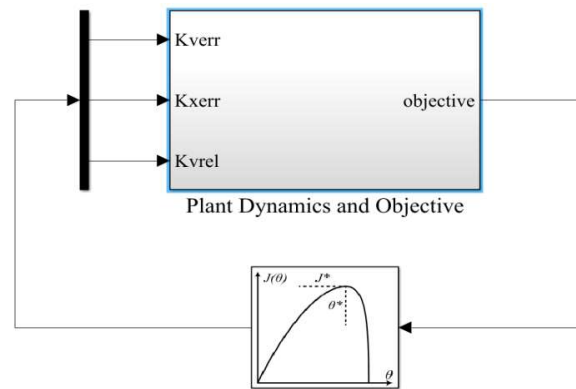


Figure 3. Simulation design of EST-based adaptive cruise controller

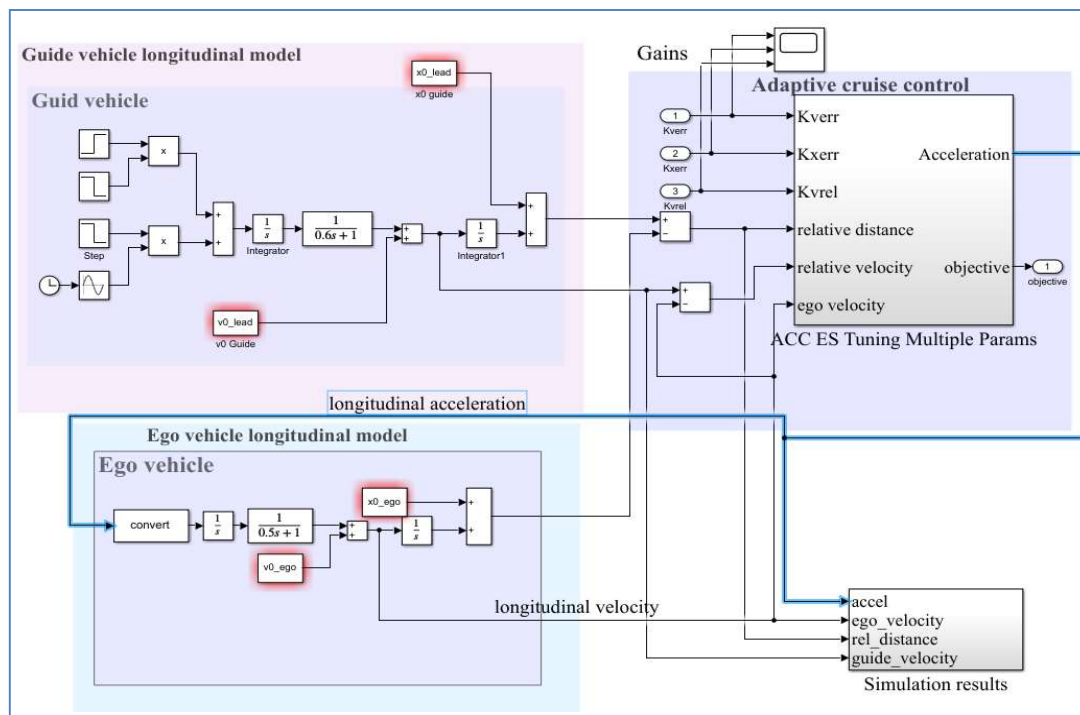


Figure 4. Simulation of the objective and plant dynamics

Table 2. Parameters of extremum seeking technique

Description	Symbol and value
Forcing frequency (rad/s)	$\omega = 0.8 * [5, 7, 8]$
ω_{hpf}	$= 0.01$
ω_{lpf}	$= 0.04$
Modulation phase (rad)	$\phi_2 = \pi/4$
Demodulation phase (rad)	$\phi_1 = 0$
Demodulation amplitude	$a = 0.01$
Modulation amplitude	$b = 0.5 * I_r$

3. RESULTS AND DISCUSSION

3.1. Velocity and relative space for guide and ego vehicles

After running the developed simulation, the result of the vehicle velocity model is shown in Figure 5(a), while the acceleration variation for the ego vehicle is shown in Figure 5(b). The ACC technique is considered to keep maintain a relatively secure space or a preferred cruising velocity from the guiding vehicle. To keep a secure in-between space the ACC technique controls the ego vehicle speed whenever the guide vehicle speed changes. When the guide vehicle velocity exceeds the set velocity with a higher value, the ego vehicle discontinues following the guide vehicle speed and cruises at the set speed. The relative space between the ego and guide vehicles with the secure distance was shown in Figure 6(a), while the relative space error between the ego and guide vehicles was shown in Figure 6(b).

The graph shows that the velocity of the guide vehicle changes in a sinusoidal pattern, which leads the ego vehicle to compensate for the difference by adjusting its speed. It is shown that the secure in-between space varies when the ego vehicle speed changes. In addition, the relative in-between space between the guide and ego vehicles irregularly falls slightly under the secure in-between space, which is due to the activity of the ACC technique to enforce the relative space to use soft restriction. The relative in-between space between the guide and ego vehicles irregularly falls slightly under the secure in-between space, which is due to the activity of the ACC technique to enforce the relative space to use soft restriction.

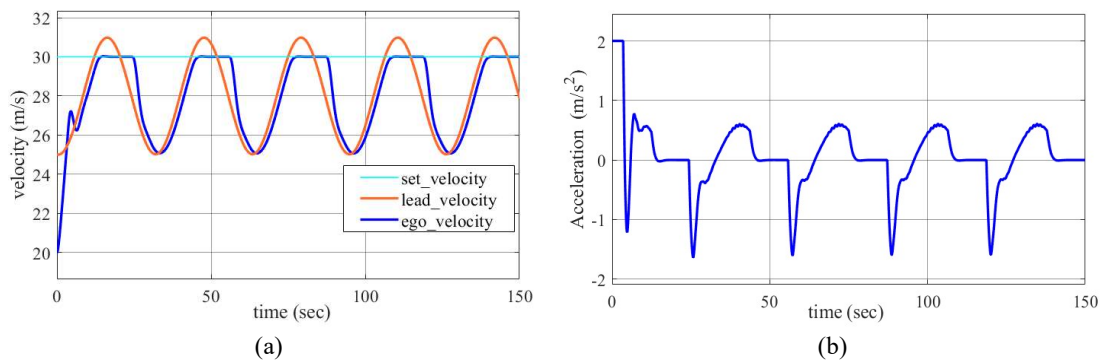


Figure 5. The model results for; (a) the velocity model for the guide and ego vehicles with the set speed and (b) the acceleration model of the ego vehicle

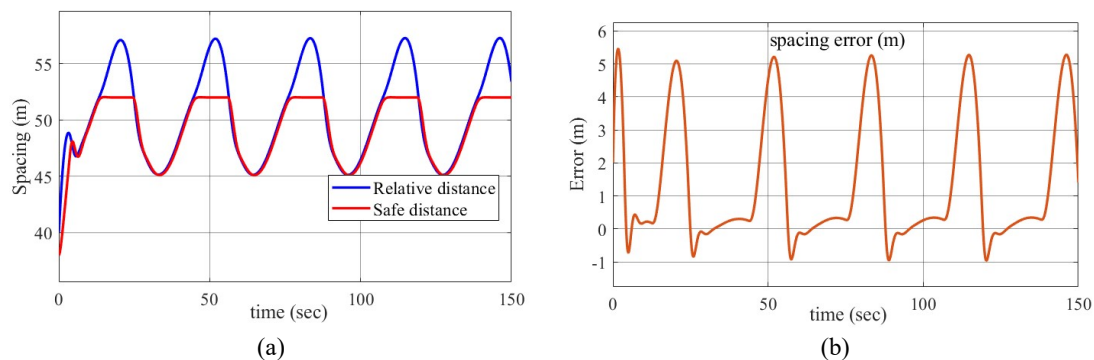


Figure 6. The relative space between the ego and guide vehicles: (a) secure distance and (b) spacing error

3.2. EST seeking cost function

The cost function is an essential parameter to determine how well the tracking model is performed for specified inputs [25]. It determines and represents as a single real number the difference between the target values and simulated values. The cost function of ESC seeking search optimization of control gains is represented in Figure 7. The cost function result shows that its values fluctuate between zero and 24 during performing the tracking process, which indicates acceptable performance.

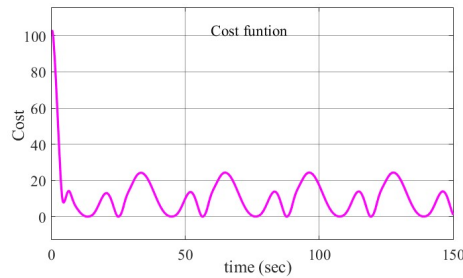


Figure 7. The costs function of ESC seeking

3.3. Controller gains

The consequential gains of controllers during tracking simulation are shown in Figure 8. The velocity error gain (K_{verr}) of the EST controller was plotted on the top followed by the position error gain (K_{xerr}) and the relative velocity gain (K_{vrel}) at the bottom. The modulation signals of the EST are what cause fluctuations in the gain values. The modulation signals of the EST are what cause fluctuations in the gain values shown in Figure 8. This fluctuation was unaffordable by this algorithm, which can be considered a type of disadvantage.

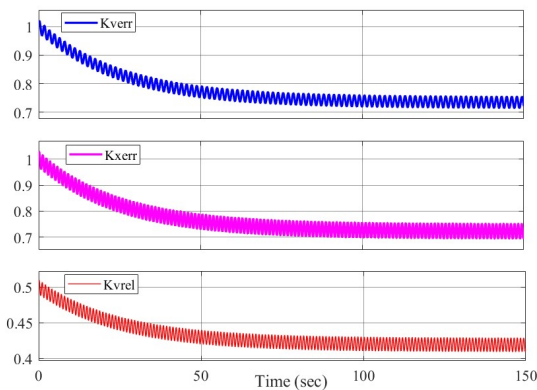


Figure 8. The gains of controllers during tracking simulation

4. CONCLUSION

This work develops an implementation of ACC by employing an EST control approach. The ego car with ACC algorithm exploits radar to determine relative velocity and relative space according to another guiding car. We can conclude the following significant points: i) the developed model for implementing the ACC by employing the EST control approach succeeded to determine the relative velocity and relative space according to the ego car to another guiding car with acceleration, not more than $\pm 2 \text{ m/s}^2$ and spacing error less than 6 m; ii) the seeking cost function of EST was decreasing to zero but with fluctuations fewer than 24 when the guide vehicle velocity was between 25–32 m/s; and iii) all the EST controller gains for the velocity error, the position error gain, and the relative velocity gain are converged to constant values with small fluctuations due to the modulation signals of EST. The limitation of this work is in its application which can be expanded in future work to cover aircraft flight control.

ACKNOWLEDGEMENTS




All authors are acknowledging the College of Engineering, the University of Diyala, Iraq for their assistance and support.

REFERENCES




- [1] A. H. Sabry, W. Z. W. Hasan, M. Zainal, M. Amran, and S. B. Shafie, "Alternative solar-battery charge controller to improve system efficiency," *Applied Mechanics and Materials*, vol. 785, pp. 156–161, 2015, doi: 10.4028/www.scientific.net/amm.785.156.
- [2] A. S. A. -Ogaili, I. B. Aris, A. Ramasamy, T. J. T. Hashim, M. B. Marsadek, and A. H. Sabry, "Integrating internal model controller (IMC) into electric vehicle charger of multiple charging mode: DC and AC fast charging," *Applied Sciences*, vol. 10, no. 12, pp. 1–22, 2020, doi: 10.3390/AP10124179.
- [3] N. A. Almamoori, B. Dziadak, and A. H. Sabry, "Design of a closed-loop autotune PID controller for three-phase for power factor corrector with Vienna rectifier," *Bulletin of Electrical Engineering and Informatics*, vol. 11, no. 4, pp. 1798–1806, 2022, doi: 10.11591/eei.v11i4.3728.
- [4] A. Rahnama, M. Xia, S. Wang, and P. J. Antsaklis, "Passivation and performance optimization using an extremum seeking co-simulation framework with application to adaptive cruise control systems," in *2016 American Control Conference (ACC)*, 2016, pp. 6109–6114, doi: 10.1109/ACC.2016.7526629.
- [5] P. J. Antsaklis *et al.*, "Control of cyberphysical systems using passivity and dissipativity based methods," *European Journal of Control*, vol. 19, no. 5, pp. 379–388, 2013, doi: 10.1016/j.ejcon.2013.05.018.
- [6] J. Zhao, X. Wang, Z. Liang, W. Li, X. Wang, and P. K. Wong, "Adaptive event-based robust passive fault tolerant control for nonlinear lateral stability of autonomous electric vehicles with asynchronous constraints," *ISA Transactions*, vol. 127, pp. 310–323, 2022, doi: 10.1016/j.isatra.2021.08.038.
- [7] T. Ma and C. Cao, "L1 adaptive output-feedback descriptor for multivariable nonlinear systems with measurement noises," *International Journal of Robust and Nonlinear Control*, vol. 29, no. 12, pp. 4097–4115, 2019, doi: 10.1002/rnc.4598.
- [8] S. Thudi and S. F. Atashzar, "Discrete windowed-energy variable structure passivity signature control for physical human-(tele) robot interaction," *IEEE Robotics and Automation Letters*, vol. 6, no. 2, pp. 3647–3654, 2021, doi: 10.1109/LRA.2021.3064204.
- [9] Z. Wang, X. Zhou, and J. Wang, "Extremum-seeking-based adaptive model-free control and its application to automated vehicle path tracking," *IEEE/ASME Transactions on Mechatronics*, vol. 27, no. 5, pp. 3874–3884, 2022, doi: 10.1109/TMECH.2022.3146727.
- [10] X. Zhong, Y. Guo, N. Li, Y. Chen, and S. Li, "Deployment optimization of UAV relay for malfunctioning base station: model-free approaches," *IEEE Transactions on Vehicular Technology*, vol. 68, no. 12, pp. 11971–11984, 2019, doi: 10.1109/TVT.2019.2947078.
- [11] D. Savitski, D. Schleinin, V. Ivanov, and K. Augsburg, "Robust continuous wheel slip control with reference adaptation: application to the brake system with decoupled architecture," *IEEE Transactions on Industrial Informatics*, vol. 14, no. 9, pp. 4212–4223, 2018, doi: 10.1109/TII.2018.2817588.
- [12] D. Zhou, A. A. -Durra, I. Matraji, A. Ravey, and F. Gao, "Online energy management strategy of fuel cell hybrid electric vehicles: a fractional-order extremum seeking method," *IEEE Transactions on Industrial Electronics*, vol. 65, no. 8, pp. 6787–6799, 2018, doi: 10.1109/TIE.2018.2803723.
- [13] J. Lin, S. Song, K. You, and C. Wu, "3-D velocity regulation for nonholonomic source seeking without position measurement," *IEEE Transactions on Control Systems Technology*, vol. 24, no. 2, pp. 711–718, 2016, doi: 10.1109/TCST.2015.2452232.
- [14] T. B. v. See, T. Meurer, and J. Greiner, "Marine boundary layer tracking using an AUV with UKF based extremum seeking," *IFAC-PapersOnLine*, vol. 54, no. 16, pp. 320–326, 2021, doi: 10.1016/j.ifacol.2021.10.111.
- [15] N. Zengin, H. Zengin, B. Fidan, and A. Khajepour, "Slip ratio optimization in vehicle safety control systems using least-squares based adaptive extremum seeking," in *Conference Proceedings - IEEE International Conference on Systems, Man and Cybernetics*, 2020, pp. 1445–1450, doi: 10.1109/SMC42975.2020.9283109.
- [16] W. Liu, X. Huo, K. Ma, and S. Chen, "Performance improvement in fast extremum seeking with adaptive phase compensator and high-gain optimizer," *IEEE Transactions on Systems, Man, and Cybernetics: Systems*, vol. 52, no. 11, pp. 6774–6788, 2022, doi: 10.1109/TSMC.2021.3098802.
- [17] D. Bhattacharjee, K. Subbarao, and K. Bhaganagar, "Extremum seeking and adaptive sampling approaches for plume source estimation using unmanned aerial vehicles," in *ALAA Scitech 2019 Forum*, 2019, pp. 1–17, doi: 10.2514/6.2019-1565.
- [18] G. Gunter *et al.*, "Are commercially implemented adaptive cruise control systems string stable?," *IEEE Transactions on Intelligent Transportation Systems*, vol. 22, no. 11, pp. 6992–7003, 2021, doi: 10.1109/TITS.2020.3000682.
- [19] A. H. Shallal, S. A. Salman, and A. H. Sabry, "Hall sensor-based speed control of a 3-phase permanent-magnet synchronous motor using a field-oriented algorithm," *Indonesian Journal of Electrical Engineering and Computer Science*, vol. 27, no. 3, pp. 1366–1374, 2022, doi: 10.11591/ijeeecs.v27.i3.pp1366-1374.
- [20] K. B. Ariyur and M. Krstić, *Real-time optimization by extremum-seeking control*. New York, NY, USA: John Wiley & Sons, 2003, doi: 10.5860/choice.41-4064.
- [21] M. Haring and T. A. Johansen, "On the accuracy of gradient estimation in extremum-seeking control using small perturbations," *Automatica*, vol. 95, pp. 23–32, 2018, doi: 10.1016/j.automatica.2018.05.001.
- [22] T. Zhang, M. Guay, and D. Dochain, "Adaptive extremum seeking control of continuous stirred-tank bioreactors," *AIChE Journal*, vol. 49, no. 1, pp. 113–123, 2003, doi: 10.1002/aic.690490111.
- [23] M. D. Sankur and D. B. Arnold, "Extremum seeking over a discrete action space," in *2021 American Control Conference (ACC)*, 2021, pp. 737–744, doi: 10.23919/ACC50511.2021.9482723.
- [24] R. Ramaraj, G. Dharmaraj, S. Srinivasan, S. Balasubramanian, M. Periyasamy, and K. Bekiroglu, "Real-time extremum seeking controller for brushless DC hub motors in electric vehicles," *IET Electric Power Applications*, vol. 14, no. 12, pp. 2438–2449, 2020, doi: 10.1049/iet-epa.2020.0117.
- [25] M. Guay, "Uncertainty estimation in extremum seeking control of unknown static maps," *IEEE Control Systems Letters*, vol. 5, no. 4, pp. 1115–1120, 2021, doi: 10.1109/LCSYS.2020.3011372.

BIOGRAPHIES OF AUTHORS






Saad A. Salman    was born in Diyala, Iraq. He received a B.Sc. degree in Electrical and Electronic Engineering, master's degree in Electrical and Electronic Engineering, and Ph.D degree in Electrical and Electronic Engineering from the University of Technology, Al-Rashied College of Engineering and Science, Baghdad, Iraq, in 1992, 1997, and 2006, respectively. He was working as the head of the Department of Computer Engineering, College of Engineering, Diyala University, Iraq from 2004 to 2012. His current research interests include control systems and applications. He has worked in various colleges, including: from 1992 to 2004, working as a lecturer at College of Engineering and Science, University of Technology, Al-Rashied, Baghdad, Iraq. From 1997 to 2000 working as an external lecturer at Department of Electrical, Technical Institute of Baquba. From 1999 to 2004 working as an external lecturer at Department of Electronic, College of Engineering, Diyala University. From 2004 to 2022 worked as a lecturer at Department of Computer Engineering, College of Engineering, Diyala University. He can be contacted at email: drsaad_eng@uodiyala.edu.iq.



Abidaoun H. Shallal    born in Diyala, Iraq, received a bachelor's and master's degree in Electrical and Electronic Engineering from Al-Rasheed College of Engineering and Science, University of Technology, Iraq in 1992 and 2001, respectively, and Ph.D. in Electrical and Electronic Engineering, Control engineering from Altinbas University, Istanbul, Turkey in 2019. He taught many subjects in his field of expertise. He has a lot of research publications in international journals. His research interests are in the field of control and robots. He can be contacted at email: abidaoun.hamdan@gmail.com.



Ahmad H. Sabry    was born in Baghdad, Iraq. He received his B.Sc. and M.Sc. degrees in Electrical and Electronics, Control and Automation, and Engineering from the University of Technology-Baghdad, Iraq, in 1994 and 2001, respectively. He received a Ph.D. degree in DC-based PV-powered home energy systems from the Department of Electrical and Electronic Engineering, Control, and Automation at UPM, Malaysia in 2017. He is the author of more than 35 articles, more than 5 inventions, and holds one patent. His research interests include integrated solar powered smart home system based on voltage matching, DC distribution, industrial robotic systems, and wireless energy management systems. He is a reviewer in more than three ISI journals. He can be contacted at email: ahs4771384@gmail.com.